

Research Articles: Systems/Circuits

Reading and modulating cortical beta bursts from motor unit spiking activity

<https://doi.org/10.1523/JNEUROSCI.1885-21.2022>

Cite as: J. Neurosci 2022; 10.1523/JNEUROSCI.1885-21.2022

Received: 17 September 2021

Revised: 1 February 2022

Accepted: 27 February 2022

This Early Release article has been peer-reviewed and accepted, but has not been through the composition and copyediting processes. The final version may differ slightly in style or formatting and will contain links to any extended data.

Alerts: Sign up at www.jneurosci.org/alerts to receive customized email alerts when the fully formatted version of this article is published.

Copyright © 2022 Bräcklein et al.

This is an open-access article distributed under the terms of the Creative Commons Attribution 4.0 International license, which permits unrestricted use, distribution and reproduction in any medium provided that the original work is properly attributed.

1 Reading and modulating cortical beta bursts from motor unit spiking
2 activity

3 Abbreviated title: Cortical and peripheral beta bursts

4 Authors

5 Mario Bräcklein¹, Deren Y Barsakcioglu¹, Alessandro Del Vecchio², Jaime Ibáñez^{1,3,4,§,*}, Dario
6 Farina^{1,§,*}

7 ¹Neuromechanics and Rehabilitation Technology Group, Department of Bioengineering, Faculty of
8 Engineering, Imperial College London, London W12 0BZ, United Kingdom

9 ²Department Artificial Intelligence in Biomedical Engineering, Friedrich-Alexander University,
10 Erlangen-Nuremberg, Erlangen, Germany.

11 ³BSICoS, IIS Aragón, Universidad de Zaragoza, Zaragoza, Spain

12 ⁴Department of Clinical and Movement Disorders, Institute of Neurology, University College London,
13 London WC1N 3BG, United Kingdom

14 * corresponding authors: d.farina@imperial.ac.uk, jibanez@iisaragon.es

15 [§]Equal contribution

16 Declaration of interests

17 DF and DYB are inventors in a patent (Neural 690 Interface. UK Patent application no. GB1813762.0.
18 August 23, 2018) and DF, DYB, JI, and MB are inventors in a patent application (Neural interface. UK
19 Patent application no. GB2014671.8. September 17, 2020) related to the methods and applications
20 of this work.

21 Acknowledgment

22 This study was supported by the EPSRC Centre for Doctoral Training in Neurotechnology and Health
23 and the European Commission grants H2020 NIMA (FETOPEN 899626). JI received the support of a
24 fellowship from "la Caixa" Foundation (ID 100010434) and from the European Union's Horizon 2020
25 research and innovation programme under the Marie Skłodowska-Curie grant agreement No 847648
26 (fellowship code is LCF/BQ/PI21/11830018).

27 Author Contribution

28 MB, JI, DYB, and DF conceived the study. MB, JI, and ADV carried out the experiments. MB
29 conducted the analysis. MB, JI, and DF interpreted the data, MB wrote and DYB, ADV, JI, and DF
30 edited the manuscript.

31 Abstract

32 Beta oscillations (13-30Hz) are ubiquitous in the human motor nervous system. Yet, their origins and
33 roles are unknown. Traditionally, beta activity has been treated as a stationary signal. However,
34 recent studies observed that cortical beta occurs in ‘bursting events’, which are transmitted to
35 muscles. This short-lived nature of beta events makes it possible to study the main mechanism of
36 beta activity found in the muscles in relation to cortical beta. Here, we assessed if muscle beta
37 activity mainly results from cortical projections. We ran two experiments in healthy humans of both
38 sexes (N=15 and N=13, respectively) to characterize beta activity at the cortical and motor unit (MU)
39 levels during isometric contractions of the tibialis anterior muscle. We found that beta rhythms
40 observed at the cortical and MU levels are indeed in bursts. These bursts appeared to be time-locked
41 and had comparable average durations (40-80ms) and rates (~3-4 bursts/second). To further confirm
42 that cortical and MU beta have the same source, we used a novel operant conditioning framework
43 to allow subjects to volitionally modulate MU beta. We showed that volitional modulation of beta
44 activity at the MU level was possible with minimal subject learning and was paralleled by similar
45 changes in cortical beta activity. These results support the hypothesis that MU beta mainly results
46 from cortical projections. Moreover, they demonstrate the possibility to decode cortical beta activity
47 from MU recordings, with a potential translation to future neural interfaces that use peripheral
48 information to identify and modulate activity in the central nervous system.

49 Significance statement

50 We show for the first time that beta activity in motor unit populations occurs in bursting events.
51 These bursts observed in the output of the spinal cord appear to be time-locked and share similar
52 characteristics of beta activity at the cortical level, such as the duration and rate at which they occur.
53 Moreover, when subjects were exposed to a novel operant conditioning paradigm and modulated
54 motor unit beta activity, cortical beta activity changed in a similar way as peripheral beta. These
55 results provide evidence for a strong correspondence between cortical and peripheral beta activity,
56 demonstrating the cortical origin of peripheral beta and opening the pathway for a new generation
57 of neural interfaces.

58 1. Introduction

59 Neural oscillations of brain activity in the beta range (13-30Hz) are ubiquitous in the motor nervous
60 system (Kilavik et al., 2013). Alongside their pervasive appearance in the brain, beta oscillations with
61 cortical origin are transmitted linearly and at fast and stable speeds to tonically active muscles
62 (Ibáñez et al., 2021; Witham et al., 2011). Beta activity can indeed represent an important portion of
63 the neural inputs received by spinal motor neurons and their innervated muscle fibres, i.e. motor
64 units (MUs) (Dideriksen et al., 2018; Farina et al., 2014; Grosse et al., 2002). However, the
65 prominence of beta activity at the MU level contrasts with the fact that, so far, it has been difficult
66 to find a direct link between these oscillations and motor function (Baker, 2007; Davis et al., 2012;
67 Engel and Fries, 2010; Jenkinson and Brown, 2011; Little et al., 2019). One aspect of beta inputs to
68 MU that makes them hard to study is not knowing which main sources are contributing to these
69 inputs. Are the characteristics of beta activity in MUs similar to the non-stationary features of beta
70 oscillations at the cortical level? Is the motor cortex the main structure projecting common beta
71 inputs to muscles? Or are there other relevant sources elsewhere in the central nervous system?

72 An interesting recent observation is that cortical beta activity is not a continuous signal, but it
73 appears in short-lived bursts (Bonaiuto et al., 2021; Feingold et al., 2015; Little et al., 2019;
74 Pfurtscheller et al., 2005; Shin et al., 2017). Such temporal non-stationary characteristics of beta
75 activity require new approaches, based on joint time and frequency analysis, to study these
76 oscillations (van Ede et al., 2018; Jones, 2016; Tal et al., 2020) and their possible links to motor
77 function (Bonaiuto et al., 2021; Little et al., 2019; Shin et al., 2017; Wessel, 2020). The tracking of the
78 non-stationary, burst-like behavior of cortical beta allows for directly following its propagation to the
79 peripheral nervous system by identifying its main characteristics, such as burst duration and
80 frequency, at the cortical and peripheral level. The analysis of the transmission of beta from the
81 central to the peripheral nervous system would provide new insights into the role of beta oscillations
82 on motor control. Moreover, understanding beta transmission would enable the development of
83 neural interfaces to monitor and extract cortical activity non-invasively from the periphery to
84 supplement and overcome current limitations of traditional brain monitoring interfaces.

85 Here we ran two experiments to characterize beta oscillations present at the level of MUs in the
86 tibialis anterior muscle and their association with cortical beta rhythms in the context of mild
87 isometric contractions. In the first experiment, we asked subjects to hold a constant force level while
88 concurrently recording cortical activity via electroencephalography (EEG) and muscle activity via
89 high-density electromyography (EMG). The EMG was decomposed into the underlying MU activity
90 associated with force generation. Then, in the second experiment, we used a decomposition
91 algorithm to extract MU activity from the EMG in real-time (Barsakcioglu et al., 2021) and a novel

92 neural feedback paradigm to operantly conditioning beta in the MUs (Bräcklein et al., 2020). By
93 doing this, we were able to assess how the relationship between cortical and peripheral beta
94 rhythms is influenced by volitional modulation of MU beta power. Overall, our results demonstrate
95 that beta activity in the MUs is short-lived, mainly driven by cortical bursts, and can be volitionally
96 modulated, imposing parallel modulation at the cortical level.

97 2. Materials and methods

98 2.1. Subjects

99 In this study, 28 healthy subjects (3 females, all subjects between 24 and 35 years old) participated,
100 of whom 15 (2 females) in Experiment 1 and 13 (1 female) in Experiment 2. All subjects were naïve
101 to the experimental paradigms. None of the subjects reported any history of severe neuronal or lower
102 limb injuries. Experiment 1 was approved by the University College London Ethics Committee (Ethics
103 Application 10037/001) and Experiment 2 by the ethics committee at Imperial College London
104 (reference number: 18IC4685).

105 2.2. Data acquisition

106 High-density surface EMG (HDsEMG) from the tibialis anterior muscle of the dominant leg (self-
107 reported) was acquired via a 64-electrode grid (5 columns and 13 rows; gold-coated; 1 mm
108 diameter; 8 mm interelectrode distance; OT Bioelettronica, Torino, Italy). The electrode grid was
109 placed over the muscle belly aligned to the muscle's fiber direction. In addition, single-channel EMG
110 of the medial and lateral head of the gastrocnemius muscle was recorded via wet electrodes (Ambu
111 Ltd, St Ives, United Kingdom) placed above the muscle belly throughout Experiment 2. The EMG
112 signals were monopolar recorded, amplified via a Quattrocento Amplifier system (OT Bioelettronica,
113 Torino, Italy), sampled at 2048Hz, A/D converted to 16 bits, and digitally band-pass filtered (10-
114 500Hz). Subjects were seated throughout the experiments while the foot of the dominant leg was
115 locked into position to allow dorsiflexion of the ankle only. The force due to ankle dorsiflexion was
116 recorded via a CCT TF-022 force transducer, amplified (OT Bioelettronica, Torino, Italy), and low-pass
117 filtered at 33Hz. The communication between the amplifier and the computer was conducted via
118 data packages of 256 samples (one buffer corresponds to a signal length of 125ms). All incoming
119 EMG signals were band-pass filtered between 20-500 Hz using a 4th order Butterworth filter.

120 Furthermore, EEG signals were acquired from 31 positions according to the International 10-
121 20 system via active Ag/AgCl electrodes (actiCAP, Brain Products GmbH, Munich, Germany). FCz was
122 used as a reference. The signal was amplified (BrainVision actiCHamp Plus, Brain Products GmbH,
123 Munich, Germany) and sampled at 1000 Hz. The EEG was offline band-pass filtered between 0.5 and
124 45 Hz (4th order Butterworth filter). A surface Laplacian filter covering the central part of the brain by
125 taking the neighboring positions of Cz into account was applied (Kayser and Tenke, 2015). Both EMG
126 and EEG signals were offline resampled at 512 Hz and synchronized with a common digital trigger
127 signal.

128 For one subject, no EMG of the lateral nor medial head of the gastrocnemius muscle was recorded
129 due to a material failure.

130 2.3. Experimental paradigm

131 The experimental paradigm for both experiments is visualized in Figure 1A.

132 2.3.1. Pre-experimental processing

133 Before the start of the experiments, subjects were asked to perform a single maximum dorsiflexion
134 of the ankle to estimate the maximum voluntary contraction level (MVC). The obtained MVC was set
135 as a reference for the following experiment to ensure that stable forces were produced by the
136 tibialis anterior muscle.

137 In addition to force feedback, Experiment 2 also informed the subjects about the amount of beta
138 activity in the MU innervating the tibialis anterior muscle. For this, an online decomposition
139 algorithm was used to decode MU activity in real-time (Barsakcioglu et al., 2021). In order to
140 estimate the separation matrix used to decode MU activity from the HDsEMG recordings, subjects
141 were instructed to perform an additional ramp and hold task. This involved a 4s period of linear
142 increase in the contraction level departing from a relaxed position and reaching a contraction level
143 of 10% of the MVC (ramp phase) and steady contraction at 10% of the MVC level held for 40s (hold
144 phase). The decomposed MU discharge behavior was visually inspected following established
145 guidelines (Del Vecchio et al., 2020) while subjects were instructed to gradually increase the force
146 due to dorsiflexion up to 10% MVC to recruit MUs.

147 2.3.2. Experiment 1 – force task

148 Experiment 1 aimed to assess the characteristics of cortical and MU beta activity during constant
149 isometric contraction at a mild force level. This experiment consisted of two blocks. In each block,
150 subjects were provided with visually guided feedback on the exerted force and asked to follow a
151 ramp and hold trajectory for 40s at 10% MVC presented on a screen while EEG was recorded
152 concurrently. Between blocks, subjects were instructed to rest to avoid muscle fatigue.

153 2.3.3. Experiment 2 – beta modulation

154 In Experiment 2, the relationship between cortical and MU beta was assessed while subjects were
155 allowed control over MU beta. For this, subjects were instructed to move a cursor inside a target
156 rectangle by exerting a force due to ankle dorsiflexion at 10% MVC. While holding the cursor inside
157 the rectangle, i.e. exerting a constant force at 10% MVC, subjects were asked to change the color of
158 the cursor to match a presented target by modulating the MU beta power at ~20Hz. Similar to
159 Experiment 1, EEG was recorded throughout Experiment 2.

160 Experiment 2 consisted of three parts: i) an *initialization phase* to determine all parameters
161 necessary for real-time neurofeedback on the MU beta activity, ii) *familiarization phase* to allow
162 subjects to get familiar with the experimental neurofeedback environment and task, and iii) the

163 *neurofeedback task* in which subjects were exposed to real-time feedback on the exerted force and
164 MU beta activity.

165 *Initialization phase*

166 The initialization phase mimicked the paradigm previously performed in (Bräcklein et al., 2020).
167 Subjects were asked to exert a force at 10% MVC for 40s guided visually by a force trajectory. During
168 this period, the underlying MU activity was used to identify the most prominent peak inside the beta
169 band of the intramuscular coherence (IMC). The IMC was used in this case as it allowed us to
170 estimate the common input to the MU pool at a given frequency (Castronovo et al., 2015; Dideriksen
171 et al., 2018). The power inside a 5Hz band of the cumulative MU spike train (CST) centered around
172 the IMC peak in the beta band was extracted online using a 3rd-order Butterworth filter. The mean of
173 this beta feature in the initial training block was used for normalization during the neurofeedback
174 part in Experiment 2. The logarithm of this normalized beta feature was then fitted to a Gaussian
175 distribution to provide feedback on the beta activity using a color code. Specifically, a blue-to-white-
176 to-red colormap was mapped to the logarithmical beta feature ranging from two standard
177 deviations below the mean (blue) to two standard deviations above the mean (red), while the mean
178 was coded via the color white (see Figure 1B). If the beta feature value was outside the range of the
179 colormap, i.e. more than two standard deviations off the mean, the displayed color was set to the
180 closest extrema (either blue or red).

181 *Familiarization phase*

182 The familiarization phase provided subjects with the same feedback environment as they
183 experienced later in the neurofeedback task. Subjects were instructed to move a cursor up into a
184 target rectangle by modulating the force exerted during dorsiflexion of the ankle. This target
185 rectangle was centered at 10% MVC with a lower and upper bound at 9.5% and 10.5% MVC,
186 respectively. The cursor's color changed accordingly to the underlying beta feature and its
187 corresponding value in the blue-white-red colourmap. If the cursor was outside the target rectangle,
188 its color was changed to black. Hence, subjects only received feedback on the underlying beta
189 feature when the cursor was inside the target. By doing this, subjects were encouraged to exert
190 stable forces. Cursor position and color were updated every 125ms. The beta feature amplitude was
191 averaged across the amplitudes observed in the seven most recent 125ms buffers analyzed as
192 previously performed by (Bräcklein et al., 2020). Subjects had approximately 10min to get
193 themselves familiar with this neurofeedback environment.

194 Neurofeedback task

195 The neurofeedback task was divided into multiple blocks. Subjects were asked to perform a
196 minimum of three and a maximum of six blocks of training before three last consecutive blocks were
197 used for further analysis. Each block consisted of three trials. Each trial started with subjects
198 contracting their tibialis anterior muscle to produce ankle dorsiflexion forces that moved the cursor
199 inside the target rectangle at 10% of the MVC. Once the cursor was within the target rectangle, the
200 force produced had to be kept constant for 30s while beta activity had to be modulated. Specifically,
201 subjects were asked to either keep the cursor blue for as long as possible (beta down-modulation
202 condition), or red (up-modulation condition). In a third condition, no feedback on the underlying
203 beta activity was given (the cursor stayed white when held inside the target; see Figure 1B). The
204 color target indicating the modulation condition of each trial, was provided verbally by the
205 experimental instructor and as visual clues by the color of the cursor edge. Hence, the cursor edge
206 was blue when subjects were asked to keep the cursor blue (down-modulating MU beta), red (up-
207 modulating beta), or black if no neurofeedback on MU beta was provided. Per block, each
208 modulation condition was presented once in a randomized order. Between each trial, subjects
209 rested for at least 1 min to minimize muscle fatigue.

210 2.4. Analysis

211 2.4.1. Spectral analysis

212 The time-frequency representation of the CST and the surface Laplacian EEG was obtained using the
213 continuous wavelet transform implemented via the `cwt` function in MATLAB (Version 2018b,
214 MathWorks Inc., MA, USA). The cortico-muscular coherence (CMC) was estimated using magnitude-
215 squared wavelet coherence implemented via the MATLAB function `wcoherence`. A similar
216 approach was chosen to estimate the temporal evolution of the IMC via a custom MATLAB script
217 built upon the `wcoherence` function. To estimate the IMC, the MU pool was split into two
218 randomly selected sub-pools of equal size. The magnitude-squared wavelet coherence between the
219 CSTs of both MU sub-pools was calculated. This step was repeated over 100 iterations, always
220 choosing a different configuration of MU sub-pools. The IMC was obtained by averaging the
221 coherence estimates obtained during the 100 iterations.

222 The beta bursting activity present in the CST and EEG signals was extracted using a band-pass filter
223 (13-30Hz, 4th-order Butterworth). The envelopes of the band-pass-filtered signals were used to
224 determine when beta bursts occurred. The threshold above which the envelope was classified as a
225 bursting event was empirically determined similar to the methods used in (Little et al., 2019; Shin et
226 al., 2017). For Experiment 1, the envelopes from EEG and CST in each block were split into 1s
227 windows. In each window, the correlation between the power of the signal and the percentage of

228 signal above the threshold was determined using the Pearson correlation coefficient and averaged
229 across blocks. Hereby, the threshold was increased from 0 to 6 times the median in .25 steps. The
230 threshold that resulted in the maximum correlation between power and percentage of signal above
231 threshold was used to identify beta events. This procedure was repeated for Experiment 2 on block-
232 level for the non-beta power feedback trials. The results are visualized in Figure 2. For Experiment 1,
233 the empirically determined threshold was 2.50 and 2.75 times the median for CST and EEG,
234 respectively. For Experiment 2, it was 2.25 and 2.75 times the median for CST and EEG. Consecutive
235 periods where the envelopes were above the threshold were marked as ON periods (beta bursting
236 events), similarly as previously performed in (Echeverria-Altuna et al., 2021). Hence, the length of
237 ON periods was used to estimate the duration of beta events. The beta event power was calculated
238 as sum of all ON events divided by the recording time. The remaining periods, i.e. when the
239 envelope was below the threshold, were identified as OFF periods. The time points of ON and OFF
240 events were set to the center of the respective periods. To analyze neural activity around ON and
241 OFF periods, the wavelet transposed spectra of CST and EEG, the wavelet CMC and IMC were
242 averaged in 500ms windows centered at the times of ON and OFF events. Furthermore, the
243 percental mismatch between ON and OFF events was calculated as: $((ON - OFF) / OFF) * 100$.

244 2.4.2. Experiment 1 – force task

245 The HDsEMG recorded during 40s of isometric ankle dorsiflexion at 10% MVC was offline
246 decomposed into the underlying MU activity using the algorithm proposed in (Negro et al., 2016).
247 The decomposition results were manually inspected as detailed in (Del Vecchio et al., 2020). To
248 control if the identified bursts in the EEG and the MU pool result from underlying amplitude
249 modulations or in contrast from isolated bursting events, the lagged coherence method was
250 employed (Fransen et al., 2015) using the NeuroDSP Python toolbox (Cole et al., 2019). This spectral
251 measure examines coherence between the signal and a delayed version of the same signal at each
252 frequency. If the lagged coherence is large, it provides evidence that the observed bursting events
253 occur in periodically and thus may be due to an underlying modulation. However, when the
254 examined signal occurs in de-coupled events, detached from any ongoing modulations, the lagged
255 coherence is smaller. The power spectral density was calculated using Welch's method (2s window,
256 50% overlap) and normalized between 1 and 40Hz.

257 2.4.3. Experiment 2 – beta modulation

258 The online decomposed MU activity was post-hoc cleaned from artefacts. Action potentials that
259 were fired with an instantaneous discharge rate above 30 spikes-per-second (sps) were neglected.
260 Only the 30s-time interval during which subjects were instructed to modulate the beta activity while
261 keeping the force constant were analyzed. In addition, the beta activity and discharge rate were

262 recalculated by neglecting MUs that had an average discharge rate below 5sps or above 30sps or a
263 discharge rate coefficient of variation (CoV) above 0.5 in any of the recorded blocks. The resulting
264 cleaned pools of MUs were used in the subsequent analysis, also for example, to recalculate the
265 beta feature and wavelet transformed CST activity, CMC, and IMC.

266 Functional values obtained during up- and down-modulation of MU beta activity, such as the mean
267 force, beta amplitude, average rectified EMG, i.e. global EMG, bipolar EMG, and the corresponding
268 CoVs to all values mentioned before, and the mean MU discharge rates were normalized by the
269 averaged values obtained during the control condition (when no neurofeedback on the MU beta
270 activity was provided). The wavelet transformed CST and EEG, CMC, and IMC were interpolated to
271 transform the logarithmical frequency scale into a linear one for further analysis to ensure an equally
272 weighted representation of all frequencies. The results were averaged inside the entire beta band
273 (13-30Hz) and within in 500ms window centered around the ON-triggered averaged. The values
274 obtained during neurofeedback were normalized by the corresponding values obtained during the
275 control condition.

276 The custom scripts used for analysis are available upon reasonable request from the corresponding
277 author.

278 2.5. Statistics

279 Statistical analysis was performed via SPSS (IBM, Armonk, NY, USA) and custom MATLAB routines.
280 Results were reported as mean \pm standard deviation. Significant clusters of beta activity in the
281 difference in the time-frequency representation of beta ON and OFF events were determined using
282 the cluster-level analysis proposed by (Maris and Oostenveld, 2007). In brief, this approach assessed
283 clusters of adjacent samples in both frequency and time dimensions under a single permutation
284 distribution (we used 10 000 permutations and an univariant clustering threshold of .05). This
285 approach allows to bypass multi-comparison issues present in multi-dimensional data. The
286 characteristics of beta bursting events in the MUs and the EEG were compared by using two-sided
287 paired t-tests. The effect of volitional beta modulation on multiple motor behavioral properties of
288 the innervated leg were tested by a repeated measures MANOVA. Hereby, the independent
289 variables were the different modulation conditions, i.e. beta down- and up-modulation. Dependent
290 variables were the mean force, mean rectified EMGs of agonist and antagonist muscles, the CoV of
291 these values and the mean discharge rates of the decomposed MUs across subjects. Differences in
292 the mean beta feature amplitude were assessed by two-sided paired t-tests. To assess whether the
293 temporal evolution of the modulated beta feature correlated with muscle activation, the correlation
294 coefficient between the exerted force, the rectified EMG of the agonist muscle or the discharge rate
295 of the identified MU pool, and the beta feature were estimated using the Pearson correlation

296 coefficient. To do this, force, rectified EMG and discharge rate were post-processed in a similar
297 fashion as the beta feature, i.e. corresponding values were averaged per each recording buffer.

298 The difference in beta event features at the cortical and MU level was assessed using linear mixed
299 models. Linear mixed models were also used to evaluate the effect of volitional beta modulation at
300 MU level on the beta bursting characteristics and spectral values, such as wavelet-transformed CST
301 and EEG, CMC, and IMC, on single blocks, in which the difference between beta down- and up-
302 modulation was the dependent variable and the subject-wise grouping a random effect. Values
303 during up- and down-modulation were normalized using data from the non-feedback condition as
304 described in 2.4.3. The partial eta-squared (η_p^2) was used to assess the effect size of the changes
305 between beta modulations. Values greater than 0.14 indicate that a “large” effect can be observed
306 in the particular comparison (Cohen, 1988). The threshold for statistical significance was set to $p <$
307 .05.

308

309 3. Results

310 3.1. Experiment 1 – force task

311 In total, 22.73 ± 7.95 MUs per block were identified in Experiment 1. Figure 3 visualizes the time-
312 frequency spectra inside the beta band of cortical (EEG signals) and muscle (the CST generated with
313 the decomposed MUs) signals during a period of isometric ankle dorsiflexion at 10% MVC. Both
314 spectra indicated that beta activity at the cortical and muscle levels occurred in short intervals, i.e.
315 bursts of activity, while subjects held constant forces. The zoomed-in plot (Figure 3, bottom)
316 suggested that some bursts observed in the muscle overlapped with bursts observed in the EEG.

317 While the observed beta burst might occur as infrequent uncoupled bursting events, they could also
318 result from an underlying amplitude-modulated oscillation. Hence, we conducted a control analysis
319 to assess whether beta bursts in MUs and EEG result from a sustained amplitude modulation. In this
320 case, the phase inside the beta band should predict the phase in upcoming cycles. In contrast, if
321 these bursts do not originate from an underlying sustained modulation, the current phase inside
322 beta should correlate less with future cycles (Fransen et al., 2015). Figure 4 illustrates that although
323 both cortical and MU show prominent beta activity in their spectra, the lagged coherence decreases
324 inside this range compared to other spectral components. Further, this effect seems prolonged
325 across multiple cycles. This indicates that in both EEG and MU activity, beta bursting events seem to
326 be isolated, thus not resulting from underlying modulation.

327 To understand activity around the short-lived beta bursts found in the EEG and CST signals, the
328 wavelet-transformed data were averaged at the center of ON and OFF periods found in the EEG
329 across blocks. Figure 5 visualizes these triggered averages for the wavelet-transformed EEG, CST, the
330 CST-EEG coherence (CMC), the intramuscular coherence (IMC), and the force profile at respective
331 time intervals. While the exerted force did not significantly change between ON and OFF periods (no
332 significant clusters, always $p > .05$), beta activity present in the EEG was significantly pronounced
333 during ON relative to OFF periods in a cluster at the center of EEG beta events ($p = .024$). Also, beta
334 activity in the CST was pronounced during ON periods compared to OFF, despite the time points of
335 ON and OFF being determined by the EEG activity ($p = .042$). It is worth noting that the maximum
336 difference between ON and OFF in the EEG was around time lag 0 (-.49ms), while the maximum
337 difference in the CST was delayed by 24.41ms. Furthermore, a significantly pronounced bursting
338 activity in the CMC was observed ($p = .001$). Similarly, the results suggested that the IMC was also of
339 transient behavior inside the beta band (IMC, $p = .026$).

340 The previous results indicated that beta activity observed in cortical and muscle recordings occurred
341 in bursts. Moreover, the significant beta activity in the CST identified during EEG beta bursting

342 events suggested that beta bursts in the MU overlapped with those present at the cortical level. This
343 confirms previous observations made using surface EMG signals (Echeverria-Altuna et al., 2021). In
344 addition, we observed that the common input inside the beta range to the MU pool was of bursting
345 behavior and appeared to be time-locked to cortical beta bursts. To further assess how beta bursts
346 observed in the MU pool matched with the beta bursts in the EEG we compared the rate and
347 duration of the beta bursts extracted from the CST and EEG (Figure 6). Beta events observed at the
348 MU level appeared at a rate of $3.56 \pm .41$ events per second while beta events in EEG at a slightly but
349 significantly lower rate of $3.23 \pm .30$ ($p = .003$, $\eta_p^2 = .469$). There was no significant difference
350 detected between the average duration of the beta bursts observed on the MU level ($55.61 \pm$
351 11.27ms) and the bursts in the EEG (53.10 ± 9.23 ; $p = .398$, $\eta_p^2 = .052$).

352 3.2. Experiment 2 – beta modulation

353 Results from Experiment 1 showed that beta activity occurs in bursts both at the cortical and muscle
354 levels. Moreover, the bursts observed at both levels are similar in features such as duration and rate
355 of events and appear to be temporarily aligned with a small offset. These results therefore support
356 the notion that beta activity in the EEG and CST have a shared underlying source. If this is the case, it
357 is expected that modulation of beta activity at the MU level should correspond to a similar
358 modulation of cortical beta observed in the EEG. To test this, Experiment 2 used a novel neural
359 interface based on real-time decomposition of MU activity from the interference EMG.

360 In this online experiment 11.92 ± 2.48 MUs per subject were identified and tracked in real time.
361 Subjects could significantly reduce the normalized mean beta amplitude during down-modulation to
362 0.91 ± 0.20 , compared to up-modulation at 1.07 ± 0.26 (two-sided paired t-test, $t(12) = -2.454$, $p =$
363 $.030$; see Figure 7A). In the context of volitional MU beta modulation, neither the mean exerted
364 force nor other functional measures of the innervated leg changed significantly (repeated measures
365 MANOVA Wilks' Lambda corrected, $p = .424$, $\eta_p^2 = .811$). Furthermore, across all subjects, no
366 temporal correlation between the beta feature and the force, rectified EMG of the tibialis anterior
367 muscle, and discharge rate of MUs were detected (Figure 7B; all medians are below the significance
368 level). Taken together, these results suggested that subjects were able to modulate the beta band
369 activity present in a MU pool without critically altering the motor output.

370 To study the impact that modulation of beta activity in the MU pool has on cortical beta activity, we
371 compared the burst power and the three burst features that contribute to the power estimate, i.e.
372 peak amplitudes of the beta bursts, the bursts durations, and the number of bursts, between beta
373 down- and up-modulation conditions normalized by the corresponding values obtained when no
374 beta feedback was provided (Figure 8). The power of the beta bursts in both CST and EEG increased

375 during up-modulation compared to down modulation from $0.89 \pm .27$ to $1.09 \pm .37$ ($p = .003$, $\eta_p^2 =$
376 $.540$) in the CST, and from $0.75 \pm .25$ to $.83 \pm .26$ ($p = .013$, $\eta_p^2 = .415$) in the EEG. The amplitudes of
377 beta bursts in the CST and in the EEG were significantly higher in the up-regulation condition than in
378 the down-modulation condition (CST: from $0.96 \pm .09$ to $1.02 \pm .12$, $p = .002$, $\eta_p^2 = .581$; EEG: from
379 $0.94 \pm .09$ to $0.96 \pm .09$, $p = .038$, $\eta_p^2 = .311$). The duration of the beta events did also change
380 between conditions at the MU level from $0.93 \pm .12$ to $1.00 \pm .11$ during down- and up-modulation,
381 respectively ($p < .001$, $\eta_p^2 = .652$) but was not significant at the cortical level with longer durations of
382 beta events during up-modulation (from $.92 \pm 0.10$ to 0.96 ± 0.11 , $p = .079$, $\eta_p^2 = .235$). The rate of
383 observed beta events at the MU level increased significantly from $0.98 \pm .15$ to $1.05 \pm .18$ ($p = .023$,
384 $\eta_p^2 = .363$). On average, the rate of beta events did also increase at the cortical from $.85 \pm .14$ to 0.89
385 $\pm .14$, but this effect was marginally not significant ($p = .058$, $\eta_p^2 = .268$).

386 The appearance of beta bursts in the EEG and MU activity changed during volitional beta feature
387 modulation. Figure 9 shows the impact of volitional beta modulation on the MU and EEG beta
388 activity during beta ON events. The spectral power in the beta band during ON events increased
389 significantly in the CST from $.99 \pm .20$ to $1.09 \pm .23$ ($p = .019$, $\eta_p^2 = .378$) and in the EEG from $.90 \pm .11$
390 to $.94 \pm .11$ ($p = .026$, $\eta_p^2 = .351$) during down- and up-modulation conditions, respectively. Similarly,
391 the IMC increased significantly during up-modulation from $0.97 \pm .06$ to $0.98 \pm .05$ ($p = .034$, $\eta_p^2 =$
392 $.321$) suggesting a stronger common input in the beta band during the up-regulation condition.
393 Interestingly, the CMC did not change significantly from $1.00 \pm .06$ to $1.00 \pm .06$ between conditions
394 ($p = .994$, $\eta_p^2 = .000$), which implies that while the common input to the MU inside the beta range
395 increased during beta up-modulation relative to down-modulation, the spectral connectivity
396 between cortical beta and MU beta remained unaffected. These results indicated that cortical beta
397 power mirrored the changes in the MU. Finally, it should be noted that the same overall effects were
398 observed when using beta bursting events in the CST to define the timing of ON periods (see Figure
399 9).

400 4. Discussion

401 We studied the correspondence of cortical beta activity with beta oscillations found in the output of
402 spinal motor neurons. To do this, we assessed how cortical and peripheral beta bursting events
403 relate to each other during muscle contractions. We then used a MU-driven neurofeedback
404 approach to modulate the beta inputs to muscles to test if cortical beta activity followed the
405 modulation of peripheral beta activity. Our results demonstrate, for the first time, that beta activity
406 present in a MU pool appears in isolated bursts that closely correspond to the beta activity observed
407 at the cortical level. In addition, when modulated at the periphery, cortical beta showed the same
408 modulation pattern. We conclude that beta activity in the periphery is mainly determined by cortical
409 projections.

410 The common beta activity present in the MU population strongly corresponded to the cortical beta
411 projections. We showed that beta activity present in a MU pool is short-lived and shares the
412 characteristics of the cortical beta rhythms, i.e. rate and duration of beta events. Moreover, the
413 common input to the MU pool inside the beta range and the resulting MU beta activity were time-
414 locked and followed cortical beta rhythms by tens of milliseconds. Although determining the
415 transmission delay by only analyzing the beta power is not robust against noise that may mask the
416 underlying shape of beta bursts, our observation is in strong agreement with previous investigations
417 using the averaged CMC (Ibáñez et al., 2021; Mima et al., 2000). When we asked subjects to perform
418 volitional modulations of the beta activity present in the MUs via a novel neurofeedback paradigm
419 (Bräcklein et al., 2020), changes in the cortical beta power were shown to be coherent with those
420 induced in the periphery. These findings suggest a strong and stable correspondence between
421 peripheral and cortical beta oscillations during steady force contractions.

422 Although the effective beta activity at the MU level could potentially result from other neural
423 centers (Thompson et al., 2019), as it was suggested to be the case for MU activity in the alpha range
424 (8-12Hz) during tremor (Christakos et al., 2006), it seems that these non-cortical contributions may
425 be minimized or suppressed in the context of cortical inputs during isometric contractions. If their
426 contribution would have superseded the presence of cortical projections at the MU level, the
427 resulting beta activity in the periphery would be expected to differ from beta patterns observed at
428 the cortical level. Moreover, the common input to the MUs inside the beta band was increased
429 during volitional up-modulation of the MU beta power while the connectivity between cortical and
430 peripheral sites remained unaffected (Figure 9). Hence, the coherence between the cortical regions
431 and the MU pool inside the beta band (CMC) did not change, but the strength of the common input
432 received by the MU pool (IMC) did. This provides additional evidence for MU beta signals mainly
433 emerging from the cortical sites: if successful beta modulation resulted from additional modulation

434 of non-cortical sources, the CMC would have been affected by the volitional beta feature modulation
435 (Negro and Farina, 2011).

436 The dominance of cortical beta inputs to muscles contrasts with the observed lack of direct influence
437 on the produced force. No significant relationship between the force output of the tibialis anterior
438 muscle and the presence of beta rhythms in the innervating MU pool was detected. Still, despite the
439 absence of any evidence for a direct link between beta bursts and the motor output, beta
440 oscillations at the MU level could determine a non-linear effect on the neural drive to the innervated
441 muscle and therefore on the force output (Watanabe and Kohn, 2015). Our results show, however,
442 that these beta events at the MU level are infrequent, i.e. approximately four events per second
443 (Figure 6). While a stationary beta that changes amplitude continuously, as simulated in (Watanabe
444 and Kohn, 2015), may influence force control, a bursting beta is very unlikely to do so since the
445 corrections in force would be far too slow to improve steadiness. Alternatively, the motor system
446 could utilize the observed beta events as a sonar signal integrating sensory information from the
447 muscle (Baker et al., 2006), yet this hypothesis requires further experimental validation. During
448 Experiment 2, when subjects were instructed to modulate MU beta power, and cortical beta
449 changed coherently, the exerted force remained unchanged. This provides further evidence that
450 apart from the timing of beta bursting events, also the modulation of the beta event amplitude does
451 lie inside a motor null-space relative to force production. Hence, the strong link between cortical and
452 spinal neurons via beta activity observed in this study did not seem to have any direct influence on
453 motor output.

454 When subjects were exposed to neurofeedback on the MU beta activity, beta modulations at the
455 cortical and MU levels were mainly driven by altering the amplitude. Also rate and duration of beta
456 events increased during beta-up modulation, however, this effect was only significant at MU level. It
457 yet remains unknown what underlying mechanism led to a volitional increase in beta power via
458 increase in the amplitude of beta bursts. One possible explanation would be that subjects were able
459 to recruit larger cortical networks involved in the projection of beta activity to the muscle. It was
460 previously shown that the duration of beta bursts was not affected by the performed motor task in
461 normal conditions (Echeverria-Altuna et al., 2021). Here, we observed, although not always
462 significant, slightly longer periods of beta events during beta up-modulation compared to down-
463 modulation of MU beta. Subjects did not receive feedback on the instantaneous amplitude of beta
464 events, nor about their duration or rate. Instead, the feedback provided on the beta feature
465 amplitude during Experiment 2 was smoothed with a moving average and aimed to motivate
466 subjects to modulate the beta activity across the entire duration of the trial, i.e. suppressing or
467 promoting beta activity as long and as often as possible. Further experiments with different

468 neurofeedback approaches (e.g., using the instantaneous behavior of beta events) are necessary to
469 investigate whether subjects could learn to modulate other characteristics of beta activity in the
470 brain and the muscles. This would be highly useful to advance our understanding of the possible
471 roles of beta oscillations in movement.

472 Finally, the strong presence of cortical projections at the MU level opens up new means of studying
473 cortical beta: peripheral neural interfaces, such as presented in (Barsakcioglu et al., 2021), would
474 allow an indirect yet reliable window into cortical activity and may contribute to an advanced
475 understanding of the functional role of beta oscillations in the human motor nervous system by
476 complementing traditional interfaces, such as based on EEG or magnetoencephalography. We
477 showed that by closing the loop with a peripheral neural interface based on MU activity, subjects
478 could volitionally modulate the power of cortical beta bursts. This could provide new possibilities to
479 exploit cortical beta, for example, as a control signal for virtual or robotic effectors (Dominijanni et
480 al., 2021; Eden et al., 2021).

481 In conclusion, we have shown for the first time that the final neural drive to muscles contains
482 bursting beta activity. Moreover, these beta bursts in the MU behavior shared the appearance and
483 were time-locked to those observed on the cortical level. Volitional modulation of MU beta activity
484 was accompanied by coherent changes in cortical beta manifesting the strong correspondence
485 between cortical and MU beta. The observed bursting activity inside the beta band appeared in
486 infrequent events at low rate and thus may, at most, influence force generation as a disturbing
487 factor rather than supporting accurate force control. Cortical beta oscillations seem to be the main
488 contribution to MU beta activity and the strong correspondence between cortical and peripheral
489 beta suggests the potential use of peripheral neural interfaces to track and modulate cortical
490 activity.

491 References

- 492 Baker, S.N. (2007). Oscillatory interactions between sensorimotor cortex and the periphery. *Curr.*
493 *Opin. Neurobiol.* *17*, 649–655.
- 494 Baker, S.N., Chiu, M., and Fetz, E.E. (2006). Afferent encoding of central oscillations in the monkey
495 arm. *J. Neurophysiol.* *95*, 3904–3910.
- 496 Barsakcioglu, D.Y., Bräcklein, M., Holobar, A., and Farina, D. (2021). Control of Spinal Motoneurons
497 by Feedback from a Non-Invasive Real-Time Interface. *IEEE Trans. Biomed. Eng.* *68*, 926–935.
- 498 Bonaiuto, J.J., Little, S., Neymotin, S.A., Jones, S.R., Barnes, G.R., and Bestmann, S. (2021). Laminar
499 dynamics of high amplitude beta bursts in human motor cortex. *Neuroimage* 118479.
- 500 Bräcklein, M., Ibanez, J., Barsakcioglu, D.Y., and Farina, D. (2020). Towards human motor
501 augmentation by voluntary decoupling beta activity in the neural drive to muscle and force
502 production. *J. Neural Eng.* *18*, 16001.
- 503 Castronovo, A.M., Negro, F., and Farina, D. (2015). Theoretical Model and Experimental Validation of
504 the estimated proportions of common and independent input to motor neurons. In 2015 37th
505 Annual International Conference of the IEEE Engineering in Medicine and Biology Society (EMBC),
506 pp. 254–257.
- 507 Christakos, C.N., Papadimitriou, N.A., and Erimaki, S. (2006). Parallel Neuronal Mechanisms
508 Underlying Physiological Force Tremor in Steady Muscle Contractions of Humans. *J. Neurophysiol.*
509 *95*, 53–66.
- 510 Cohen, J. (1988). *Statistical Power Analysis for the Behavioral Sciences*. (Hillsdale, NJ: Lawrence
511 Erlbaum Associates, Publishers), p. 567.
- 512 Cole, S., Donoghue, T., Gao, R., and Voytek, B. (2019). NeuroDSP: A package for neural digital signal
513 processing. *J. Open Source Softw.* *4*, 1272.
- 514 Davis, N.J., Tomlinson, S.P., and Morgan, H.M. (2012). The Role of Beta-Frequency Neural
515 Oscillations in Motor Control. *J. Neurosci.* *32*, 403–404.
- 516 Dideriksen, J.L., Negro, F., Falla, D., Kristensen, S.R., Mrachacz-Kersting, N., and Farina, D. (2018).
517 Coherence of the Surface EMG and Common Synaptic Input to Motor Neurons. *Front. Hum.*
518 *Neurosci.* *12*, 207.
- 519 Dominijanni, G., Shokur, S., Salvietti, G., Buehler, S., Palmerini, E., Rossi, S., De Vignemont, F.,
520 d’Avella, A., Makin, T.R., Prattichizzo, D., et al. (2021). The neural resource allocation problem when

- 521 enhancing human bodies with extra robotic limbs. *Nat. Mach. Intell.* 2021 310 3, 850–860.
- 522 Echeverria-Altuna, I., Quinn, A.J., Zokaei, N., Woolrich, M.W., Nobre, A.C., and Van Ede, F. (2021).
523 Transient beta activity and connectivity during sustained motor behaviour. *BioRxiv*
524 2021.03.02.433514.
- 525 van Ede, F., Quinn, A.J., Woolrich, M.W., and Nobre, A.C. (2018). Neural Oscillations: Sustained
526 Rhythms or Transient Burst-Events? *Trends Neurosci.* 41, 415.
- 527 Eden, J., Bräcklein, M., Pereda, J.I., Barsakcioglu, D.Y., Di Pino, G., Farina, D., Burdet, E., and Mehring,
528 C. (2021). Human movement augmentation and how to make it a reality. *ArXiv Prepr.*
- 529 Engel, A.K., and Fries, P. (2010). Beta-band oscillations — signalling the status quo? *Curr. Opin.*
530 *Neurobiol.* 20, 156–165.
- 531 Farina, D., Negro, F., and Dideriksen, J.L. (2014). The effective neural drive to muscles is the common
532 synaptic input to motor neurons. *J. Physiol.* 592, 3427–3441.
- 533 Feingold, J., Gibson, D.J., DePasquale, B., and Graybiel, A.M. (2015). Bursts of beta oscillation
534 differentiate postperformance activity in the striatum and motor cortex of monkeys performing
535 movement tasks. *Proc. Natl. Acad. Sci.* 112, 13687–13692.
- 536 Fransen, A.M.M., van Ede, F., and Maris, E. (2015). Identifying neuronal oscillations using
537 rhythmicity. *Neuroimage* 118, 256–267.
- 538 Grosse, P., Cassidy, M.J., and Brown, P. (2002). EEG–EMG, MEG–EMG and EMG–EMG frequency
539 analysis: physiological principles and clinical applications. *Clin. Neurophysiol.* 113, 1523–1531.
- 540 Ibáñez, J., Vecchio, A. Del, Rothwell, J.C., Baker, S.N., and Farina, D. (2021). Only the Fastest
541 Corticospinal Fibers Contribute to β Corticomuscular Coherence. *J. Neurosci.* 41, 4867–4879.
- 542 Jenkinson, N., and Brown, P. (2011). New insights into the relationship between dopamine, beta
543 oscillations and motor function. *Trends Neurosci.* 34, 611–618.
- 544 Jones, S.R. (2016). When brain rhythms aren't 'rhythmic': implication for their mechanisms and
545 meaning. *Curr. Opin. Neurobiol.* 40, 72–80.
- 546 Kayser, J., and Tenke, C.E. (2015). On the benefits of using surface Laplacian (current source density)
547 methodology in electrophysiology. *Int. J. Psychophysiol.* 97, 171–173.
- 548 Kilavik, B.E., Zaepffel, M., Brovelli, A., MacKay, W.A., and Riehle, A. (2013). The ups and downs of
549 beta oscillations in sensorimotor cortex. *Exp. Neurol.* 245, 15–26.

- 550 Little, S., Bonaiuto, J., Barnes, G., and Bestmann, S. (2019). Human motor cortical beta bursts relate
551 to movement planning and response errors. *PLOS Biol.* *17*, e3000479.
- 552 Maris, E., and Oostenveld, R. (2007). Nonparametric statistical testing of EEG- and MEG-data. *J.*
553 *Neurosci. Methods* *164*, 177–190.
- 554 Mima, T., Steger, J., Schulman, A.E., Gerloff, C., and Hallett, M. (2000). Electroencephalographic
555 measurement of motor cortex control of muscle activity in humans. *Clin. Neurophysiol.* *111*, 326–
556 337.
- 557 Negro, F., and Farina, D. (2011). Decorrelation of cortical inputs and motoneuron output. *J.*
558 *Neurophysiol.* *106*, 2688–2697.
- 559 Negro, F., Muceli, S., Castronovo, A.M., Holobar, A., and Farina, D. (2016). Multi-channel
560 intramuscular and surface EMG decomposition by convolutive blind source separation. *J. Neural Eng.*
561 *13*, 26027.
- 562 Pfurtscheller, G., Neuper, C., Brunner, C., and da Silva, F.L. (2005). Beta rebound after different types
563 of motor imagery in man. *Neurosci. Lett.* *378*, 156–159.
- 564 Shin, H., Law, R., Tsutsui, S., Moore, C.I., and Jones, S.R. (2017). The rate of transient beta frequency
565 events predicts behavior across tasks and species. *Elife* *6*, 6:e29086.
- 566 Tal, I., Neymotin, S., Bickel, S., Lakatos, P., and Schroeder, C.E. (2020). Oscillatory Bursting as a
567 Mechanism for Temporal Coupling and Information Coding. *Front. Comput. Neurosci.* *0*, 82.
- 568 Thompson, C.K., Johnson, M.D., Negro, F., Mcpherson, L.M., Farina, D., and Heckman, C.J. (2019).
569 Exogenous neuromodulation of spinal neurons induces beta-band coherence during self-sustained
570 discharge of hind limb motor unit populations. *J. Appl. Physiol.* *127*, 1034–1041.
- 571 Del Vecchio, A., Holobar, A., Falla, D., Felici, F., Enoka, R.M., and Farina, D. (2020). Tutorial: Analysis
572 of motor unit discharge characteristics from high-density surface EMG signals. *J. Electromyogr.*
573 *Kinesiol.* *53*, 102426.
- 574 Watanabe, R.N., and Kohn, A.F. (2015). Fast Oscillatory Commands from the Motor Cortex Can Be
575 Decoded by the Spinal Cord for Force Control. *J. Neurosci.* *35*, 13687 LP – 13697.
- 576 Wessel, J.R. (2020). β -Bursts Reveal the Trial-to-Trial Dynamics of Movement Initiation and
577 Cancellation. *J. Neurosci.* *40*, 411.
- 578 Witham, C.L., Riddle, C.N., Baker, M.R., and Baker, S.N. (2011). Contributions of descending and
579 ascending pathways to corticomuscular coherence in humans. *J. Physiol.* *589*, 3789–3800.

580 Figure legends

581 **Figure 1: Schematic overview of the experimental paradigms used in both experiments.** A: Experimental flow-chart for
 582 Experiment 1 and 2. Both experiments start with estimating the maximum voluntary contraction level (MVC). In Experiment
 583 1, subjects are asked to repeat two blocks of ramp-and-hold force task at 10% MVC separated by a rest period. Experiment
 584 2 continues with two initialization steps in which the online decomposition (“Initialization online decomposition”) and the
 585 neurofeedback parameters (“Initialization phase”) are initialized. In “Familiarization phase” subjects are exposed to the
 586 neurofeedback paradigm used during the “Neurofeedback task”. A single block of the “Neurofeedback task” consisted of
 587 three trials: beta down, beta up, and control. The trials were presented in randomized order and separated by a rest period.
 588 A minimum of six and a maximum of nine blocks were presented to each subject separated by a rest period while only the
 589 last three blocks were used for the analysis. B: Schematic overview of Experiment 2. HDsEMG of the tibialis anterior muscle
 590 was decomposed into the underlying neural activity while, concurrently, the force due to ankle dorsiflexion and the EEG
 591 were recorded. Subjects were asked to navigate a cursor inside a target rectangle by performing ankle dorsiflexion at $10\% \pm$
 592 $.5\%$ MVC. Color of the cursor changed based on the beta power in the MU pool. Subjects were asked to keep the cursor
 593 inside the force target and change the cursor color to either blue (down-modulation of the beta activity) or red (up-
 594 modulation of the beta activity). In a control condition, no feedback on the beta feature was provided and, instead, the
 595 cursor turned white when placed inside the target.

596 **Figure 2: Beta burst threshold estimation.** Correlation between beta band power and number of samples above threshold
 597 for Experiment 1 (top) and Experiment 2 (bottom) for the MU (left) and EEG (right) data. Grey lines indicate single blocks
 598 while solid black line indicate mean across blocks. For Experiment 2, only the control condition was used. Dashed black lines
 599 indicate maximum correlation value and corresponding threshold.

600 **Figure 3: Beta power present in the EEG and MU pool shown in a representative subject.** TOP: Force due to dorsiflexion of
 601 the ankle, interpolated time-frequency spectrum inside the beta band for surface Laplacian EEG and CST via continuous
 602 wavelet transform. BOTTOM: Zoom-into force, interpolated time-frequency-spectra of surface Laplacian EEG and CST, and
 603 beta band power (blue) and maxima envelope (red) extracted from the band-pass filtered CST. The Black dashed line
 604 indicates the threshold used to identify beta bursts (ON, grey shaded areas) and valleys in between bursts (OFF).

605 **Figure 4: Lagged coherence analysis for EEG (left) and MU activity (right).** Top: Mean power spectral density normalized
 606 between 1 and 40Hz across all blocks. Shaded areas indicate standard error of the mean. Middle: Mean lagged coherence
 607 at three cycles across all blocks. Shaded areas indicate standard error of the mean. Bottom: Mean lagged coherence for
 608 cycles 3 to 7 across blocks.

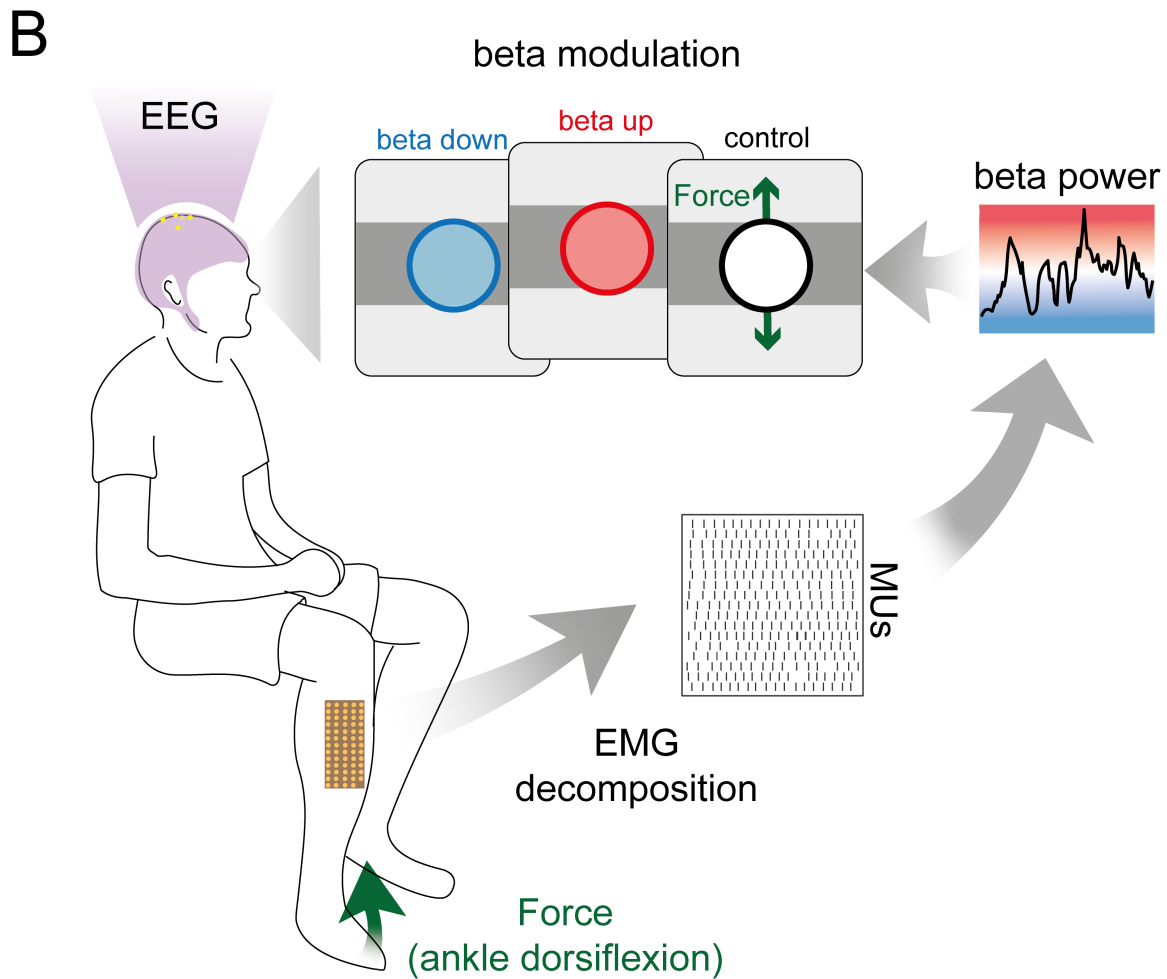
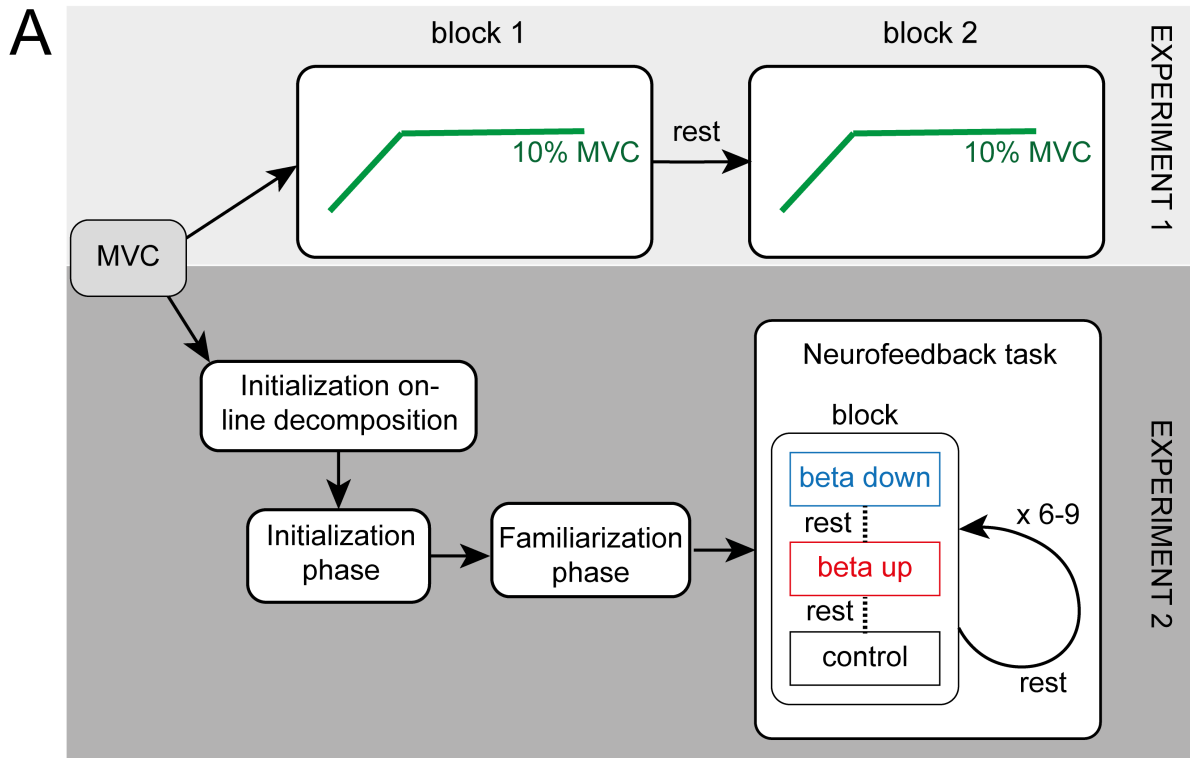
609 **Figure 5: Neural activity during beta bursting events present in the EEG.** ON and OFF periods were aligned and averaged
 610 across blocks. From top row to bottom: force (shading indicates 95% percentile), interpolated wavelet-transformed EEG,
 611 wavelet-transformed-MU activity, CMC, and IMC, at the center time points of ON periods (left), OFF periods (center), and
 612 percental mismatch (right). Black boundaries indicate significant clusters ($p < .05$).

613 **Figure 6: Relationship between beta bursts observed at the cortical and muscle levels.** The rate at which beta events
 614 occurred (left) and their mean duration (right) are shown for cortical (EEG) and peripheral (CST) signals across blocks by
 615 their median and quantiles. Values for individual blocks are marked in grey and connected observation sides of beta events
 616 (i.e. CST and EEG). $**p < .01$

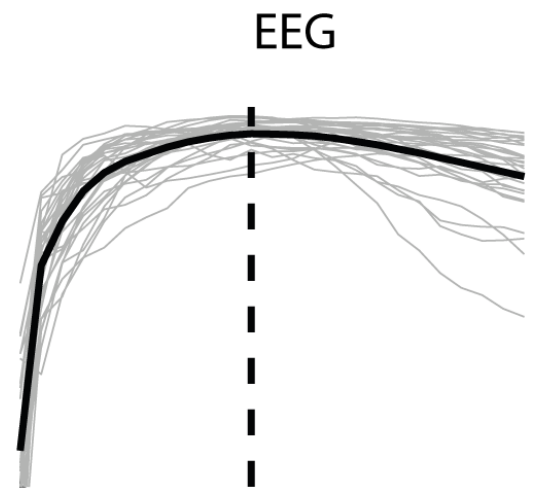
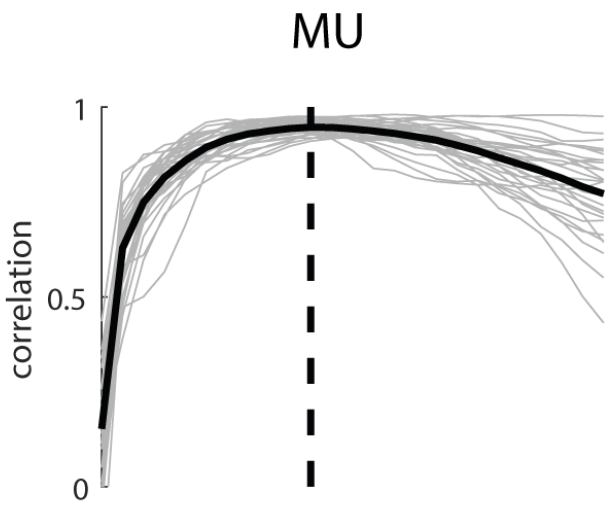
617 **Figure 7: Functional values during beta power modulation.** A: Mean force and beta feature amplitude (normalized by
618 mean amplitude during non-feedback condition) during down- and up-modulation conditions (blue and red, respectively)
619 shown by their median and quantiles all subjects. Grey points indicate the mean value per subject, while grey lines combine
620 data of the same subject. * $p < .05$. B: Temporal correlation between the beta power feature and the force, global EMG of
621 the tibialis anterior and the mean discharge rate (DR) shown across subjects with their median and quantiles. Black bar
622 indicates significance level of correlation.

623 **Figure 8: Normalized beta events features during modulation.** Mean power, amplitude, duration and rates of beta events
624 are shown across blocks. Corresponding values for beta down-modulation (blue), and up-modulation (red) are normalized
625 by the control condition (no neurofeedback on beta activity). The top row shows values observed on the MU level (CST) and
626 the bottom one for EEG level. Grey dots indicate values for single blocks. Grey lines combine values corresponding to the
627 same block. * $p < .05$

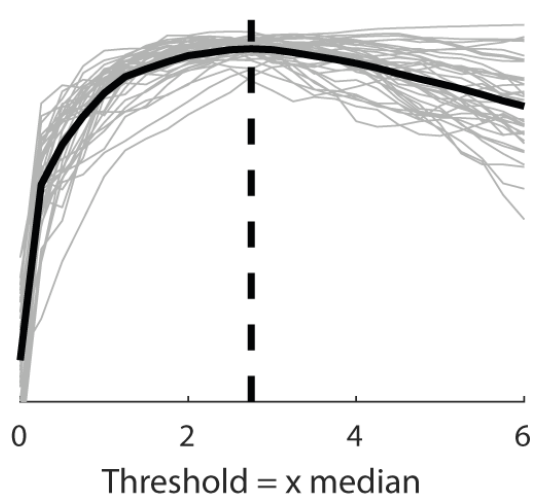
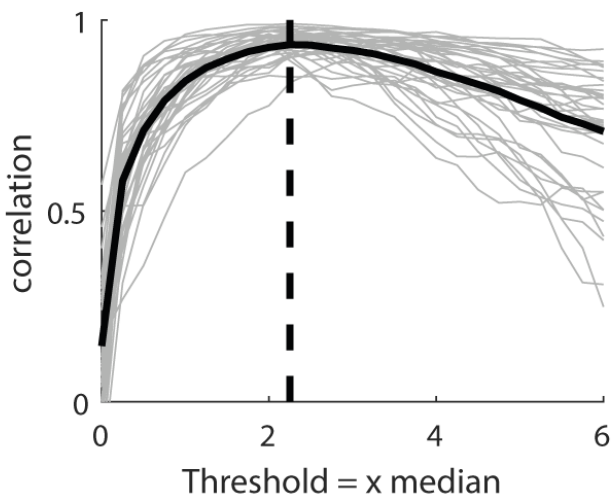
628 **Figure 9: Impact of volitional beta feature modulation on spectral measures.** From left to right: beta band power
629 extracted from the MU activity and EEG, beta-band coherence in the CMC and IMC across subjects during beta feature
630 down- (blue) and up-modulation (red). Mean values were extracted from a 500ms window centered around the ON periods
631 identified in the EEG (top) and MU activity (CST, bottom) and were normalized by the corresponding values obtained during
632 the control condition (no beta neurofeedback). Grey dots indicate values for single block, while grey lines combine values
633 corresponding to the same block. * $p < .05$

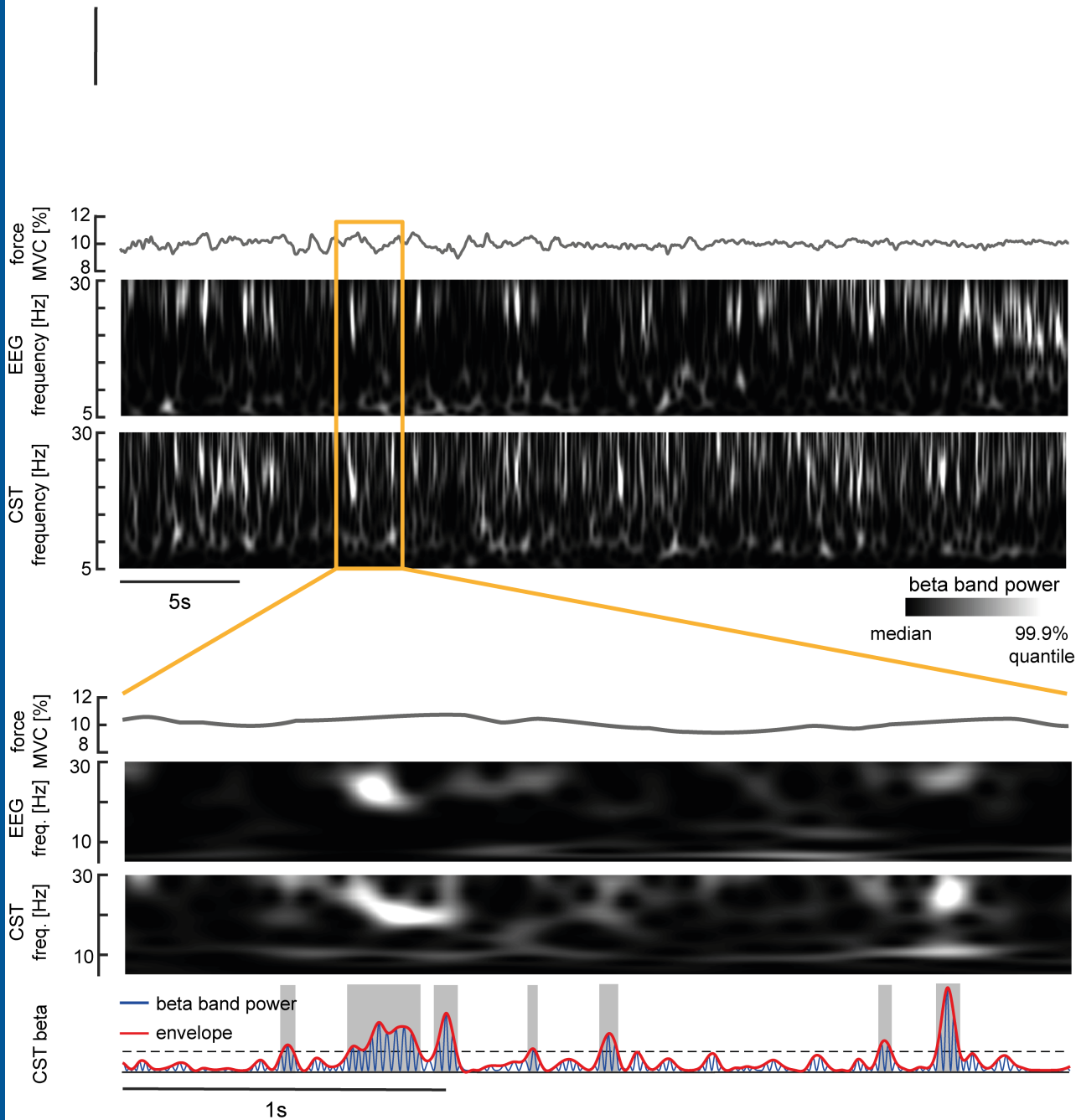


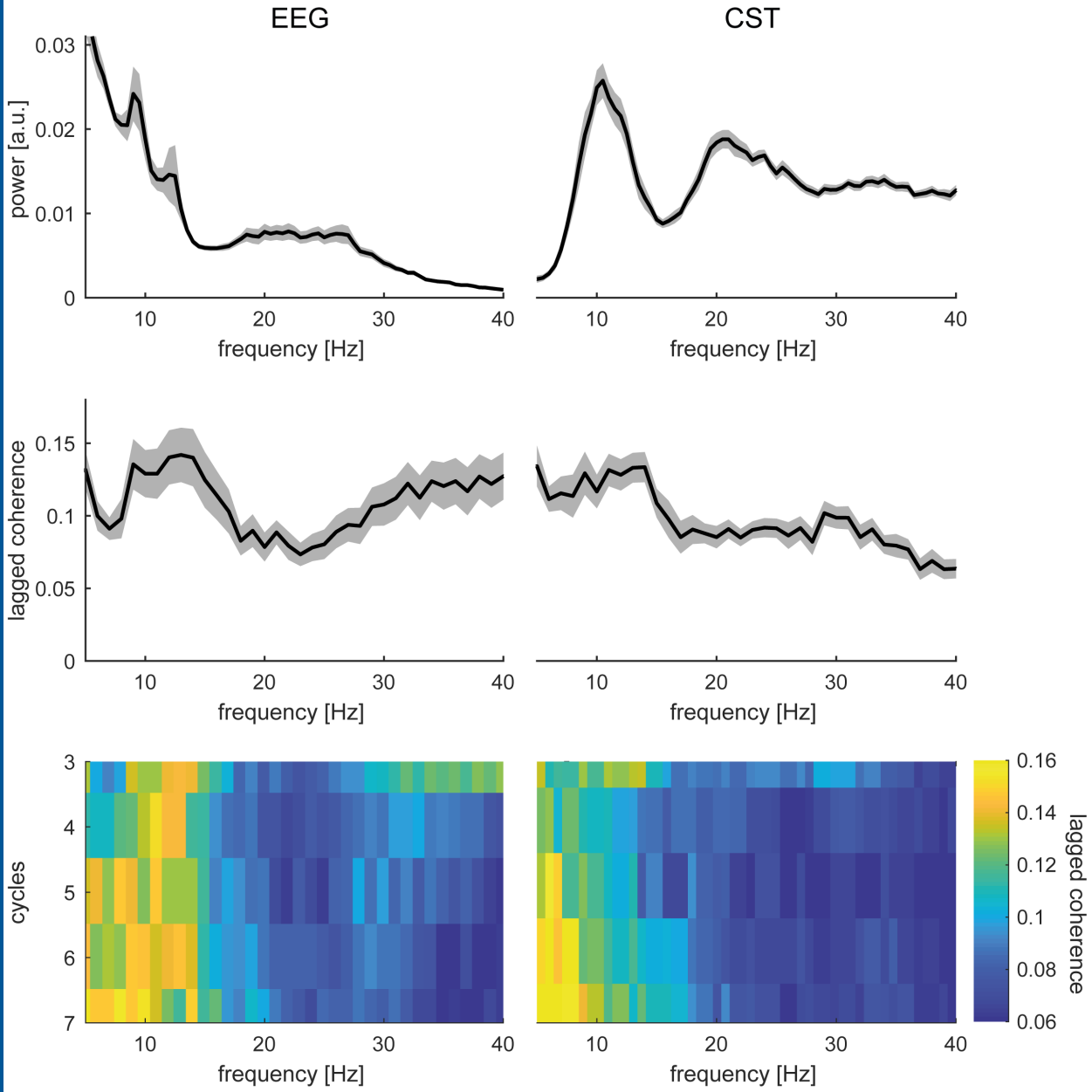
Experiment 1

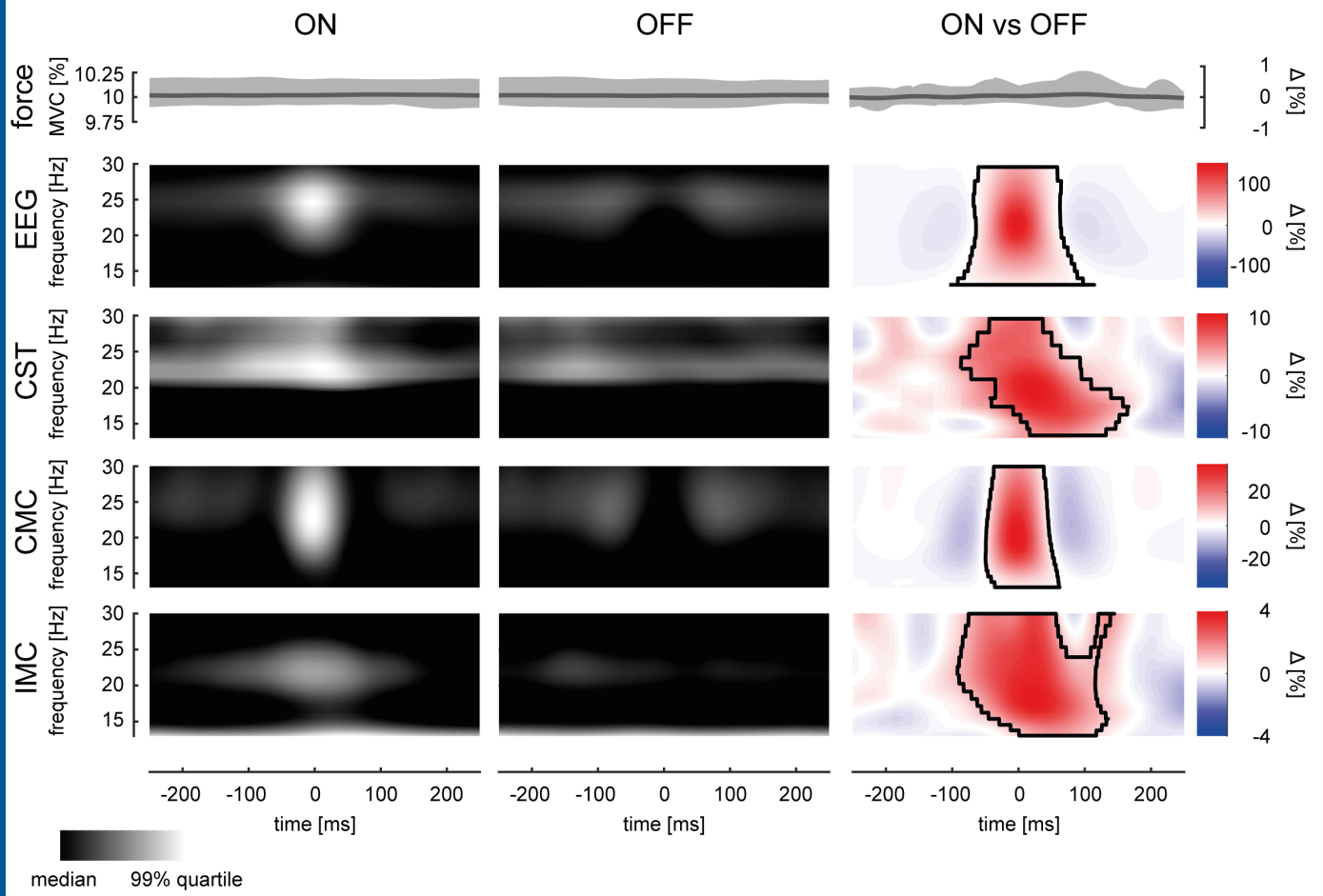


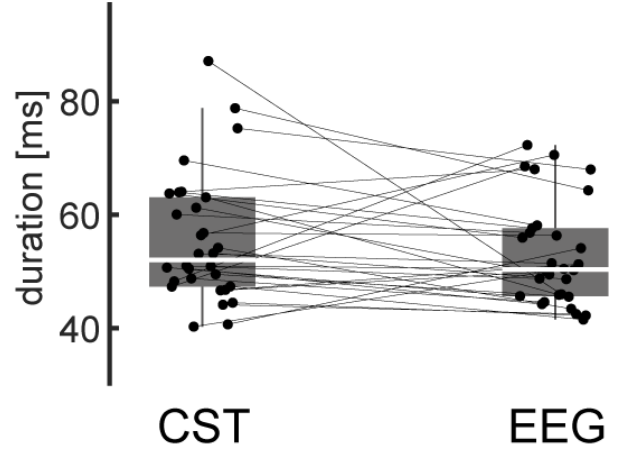
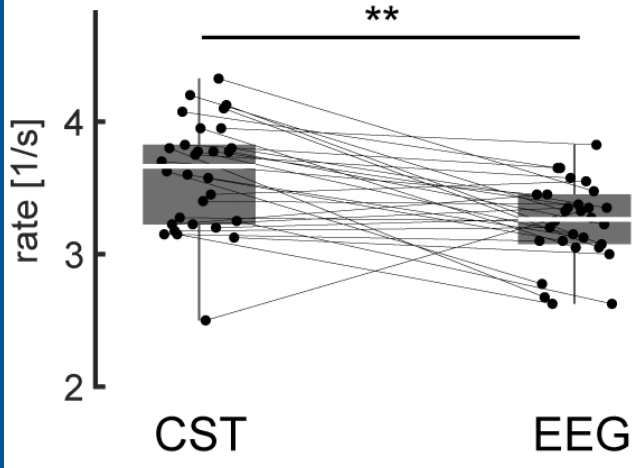
Experiment 2



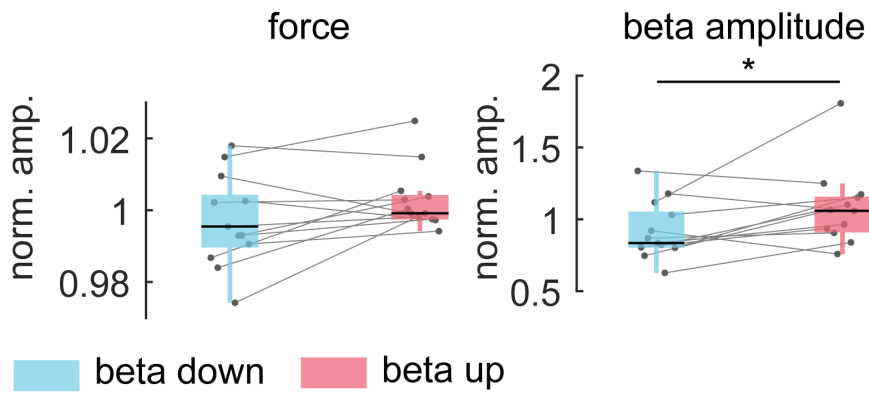




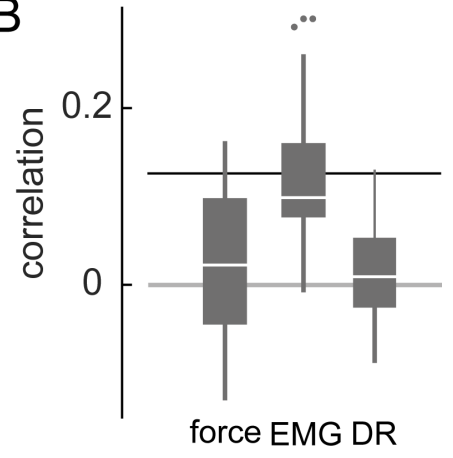




A



B





CST

